HHS Public Access

Author manuscript

Biochim Biophys Acta. Author manuscript; available in PMC 2020 April 14.

Published in final edited form as:

Biochim Biophys Acta. 2016 June ; 1860(6): 1317–1325. doi:10.1016/j.bbagen.2016.03.020.

Contribution of inorganic polyphosphate towards regulation of mitochondrial free calcium

M.E. Solesio[a], **L. Demirkhanyan**[b], **E. Zakharian**[b], **E.V. Pavlov**[a,*]

[a]Department of Basic Sciences, New York University College of Dentistry, 345 East 24th Street, 10010 New York, NY, USA

[b]Department of Cancer Biology and Pharmacology, 1 Illini Drive, 61605 Peoria, IL, USA

Abstract

Background: Calcium signaling plays a key role in the regulation of multiple processes in mammalian mitochondria, from cellular bioenergetics to the induction of stress-induced cell death. While the total concentration of calcium inside the mitochondria can increase by several orders of magnitude, the concentration of bioavailable free calcium in mitochondria is maintained within the micromolar range by the mitochondrial calcium buffering system. This calcium buffering system involves the participation of inorganic phosphate. However, the mechanisms of its function are not yet understood. Specifically, it is not clear how calcium-orthophosphate interactions, which normally lead to formation of insoluble precipitates, are capable to dynamically regulate free calcium concentration. Here we test the hypothesis that inorganic polyphosphate, which is a polymerized form of orthophosphate, is capable to from soluble complexes with calcium, playing a significant role in the regulation of the mitochondrial free calcium concentration.

Methods: We used confocal fluorescence microscopy to measure the relative levels of mitochondrial free calcium in cultured hepatoma cells (HepG2) with variable levels of inorganic polyphosphate (polyP).

Results: The depletion of polyP leads to the significantly lower levels of mitochondrial free calcium concentration under conditions of pathological calcium overload. These results are coherent with previous observations showing that inorganic polyphosphate (polyP) can inhibit calcium-phosphate precipitation and, thus, increase the amount of free calcium.

Conclusions: Inorganic polyphosphate plays an important role in the regulation of mitochondrial free calcium, leading to its significant increase.

General significance: Inorganic polyphosphate is a previously unrecognized integral component of the mitochondrial calcium buffering system.

*Corresponding author. ep37@nyu.edu (E.V. Pavlov).

Transparency document

The Transparency document associated with this article can be found, in online version.

Appendix A. Supplementary data

Supplementary data to this article can be found online at http://dx.doi.org/10.1016/j.bbagen.2016.03.020.

Keywords

Inorganic polyphosphate; Mitochondria; Calcium; Polyphosphatase

1. Introduction

Calcium is a versatile secondary messenger that plays a key role in many different physiological signaling pathways [1,2]. In addition to its essential role in cell physiology, calcium is also a key participant in cell death. When its concentration and flux inside the cells are not properly maintained, calcium can trigger either necrotic or apoptotic cell death [reviewed in [3]].

Free calcium concentration is not constant in all cell compartments. For example, in the cytoplasm, the concentration of this ion is approximately 100 nM while in the extracellular space it reaches values in the range of 1 mM. Keeping these calcium gradients between the cytoplasm and the different cell compartments is essential for the maintenance of the proper cell homeostasis. In this process, mitochondria and endoplasmic reticulum (ER) are the two organelles critically involved, [reviewed in [4]]. In these organelles, the concentration of free (that is, bioavailable) calcium is regulated not only by membrane transport but also by calcium buffering processes. In fact, during physiological and pathological calcium signaling events, both mitochondria and ER can accumulate significant amounts of total calcium, while maintaining relatively low, micromolar levels of free calcium concentration.

While in the ER the buffering mechanism is well-established and it is provided by the calsequestrins [reviewed in [5]], a family of specialized calcium buffering proteins, in mitochondria no specialized calcium binding proteins has been found and it is generally believed that the role of calcium buffering is played by orthophosphate [6–8]. Importantly, it has been established that simple orthophosphate-calcium interactions cannot explain mitochondrial calcium buffering properties. Thus, it has been postulated that other forms of phosphate should play an essential role in this process [9].

Under standard physiological conditions the mitochondrial calcium buffering capacity, expressed as a ratio between total and free calcium, is estimated to be 30,000 [10,11], while under pathological calcium uptake conditions, the ratio between bound and free calcium can reach levels as high as 150,000 [9]. These numbers show the importance of mitochondrial calcium buffering. In fact, dysfunctions in the calcium handling capability of these organelle are believed to be the basis of many disorders, including neurodegenerative processes, [12–14], cancer [15,16] and heart diseases [17,18].

Here we hypothesized that long-chain inorganic polyphosphate (polyP) plays a significant role in the regulation of the levels of free calcium in mitochondria. PolyP is a polymerized form of inorganic orthophosphate that is present in mitochondria in the length of up to 100 monomers. PolyP is one of the most ancient and well-conserved molecules and is widespread in all living beings. In fact, polyP is found in all mammalian cells, forming chains of different lengths and performing a broad range of functions [19–23]. The total amount of cellular polyP is highly variable and it depends on specific human tissues and

cells. For example, in unstimulated osteoblast-like cells, the total concentration of polyP was shown to be around 500 μM (estimated as orthophosphate residues), while in human blood plasma cells, it is 10-folds lower and in gingival cells, erythrocytes, and peripheral blood mononuclear cells it is estimated to be between 3 and 6 times lower. On the other hand, in platelets the concentration of polyP it is supposed to be within the millimolar range [24,25]. Generally, in mammalian organelles polyP is estimated to be within the μM range, usually between ten and several hundred μM [26]. Regarding the physiological functions of polyP, it has been previously demonstrated that this polymer is involved in the process of bone mineralization, through the modulation of the calcium-orthophosphate interactions [24,27]. Moreover, in the case of the mammalian mitochondria, polyP has been shown to be linked to the energy metabolism [28] and ion channel activity [29–32]. However, its potential role in the regulation of free mitochondrial calcium concentration, $[Ca^{2+}]_{mito\text{-}free}$, has never been addressed before. Here we found that during acute calcium overload, the presence of polyP leads to increased levels of $[Ca^{2+}]_{mito\text{-}free}$. We hypothesize that PolyP will increase $[Ca^{2+}]_{mito\text{-}free}$, due to its ability to modulate calcium interactions with orthophosphate and/or other forms of endogenous phosphates.

2. Results

2.1. Localization and relative amount of polyP in differentiated and undifferentiated HepG2 cells

HepG2 cells represent a well-established model for calcium signaling studies [33–35]. Furthermore, differentiated HepG2 cells are characterized by increased levels of expression of alkaline phosphatase [36], which is a potent polyP hydrolyzing enzyme in different mammalian systems [37–41]. Thus, we hypothesized that differentiated HepG2 cells will have different levels of polyP, comparing to the undifferentiated ones. This characteristic will provide us with a model suitable for investigate the contribution of polyP towards calcium regulation. To test this, we cultured both cell types. Undifferentiated HepG2 cells grew in clusters, showing a round shape (Fig. 1A). At approximately 50% of confluence, these cells started to form aggregates impossible to segregate by using trypsin. For this reason, we kept confluence under 50%. After differentiation, morphological changes were observed. Specifically, differentiated cells became more elongated and were able to reach higher levels of confluence, without forming aggregates (Fig. 1B). The levels of alkaline phosphatase present in both differentiated and undifferentiated HepG2 cells, as well as in differentiated and undifferentiated SH-SY5Y cells, were measured by Western Blot analysis. While we found an increment in the signal in HepG2 differentiated cells, no differences were found in SH-SY5Y cells (Fig. 1C and Supplementary Fig. 5B, respectively).

Next, we investigated the levels and the intracellular distribution of polyP in both cell types. To do this, we used an immunocytochemical approach, based on the affinity of the recombinant Poly-Phosphate Binding Domain (PPBD) of Escherichia coli exopolyphosphatase to polyP [42]. When applied to the fixed cells, this domain selectively recognizes polyP, which can be visualized by fluorescent antibodies, using a confocal microscope. To specifically assay the changes in polyP levels in mitochondria, we selectively measured PPBD fluorescence at the mitochondrial regions. Mitochondrial

regions were identified using antibodies against TOMM20, a classical mitochondrial marker. Fig. 2C shows the result of the analysis of the fluorescence profile (Fig. 2B) collected from the image in Fig. 2A. By using this PPBD probe we have found that the amount of polyP showing mitochondrial localization is decreased after HepG2 cells differentiation, (fluorescence AU 82 ± 4 vs. 51 ± 5, $p < 0.001$). Combined outcome of three independent experiments is shown in Supplementary Fig. 1. Interestingly, in addition to the changes in the polyP in mitochondria, we also found considerable differences in polyP distribution in the regions not related to mitochondria. Specifically, we found an apparent decrease in the levels of polyP in the cytoplasm (note the disappearance of the non-mitochondrial granular structures in differentiated cells). On the other hand, we found a dramatic increase in the levels of polyP in the nuclei, after cells were differentiated.

2.2. $[Ca^{2+}]_{mito\text{-}free}$ levels in differentiated and undifferentiated HepG2 cells, under conditions of acute overload

Maintaining an appropriate $[Ca^{2+}]_{mito\text{-}free}$ inside mitochondria during stress is critical for cell survival. To investigate the contribution of polyP to the regulation of $[Ca^{2+}]_{mito\text{-}free}$ under conditions of calcium overload we used ionomycin, a well-known calcium ionophore [43]. Ionomycin, induces calcium load independently of any transporter or other import mechanisms and, thus, allows us to directly assessing calcium buffering, while excluding potential effects of channels and mitochondrial metabolic state. Importantly, this loading does not depend on mitochondrial membrane potential [44], as was confirmed by the lack of changes in Rhod-2 fluorescence after the addition of depolarizing concentration of FCCP to cells already treated with ionomycin (Supplementary Fig. 3).

Real-time experiments using live HepG2 cells and the mitochondrial calcium indicator Rhod-2 AM showed that the addition of ionomycin increased $[Ca^{2+}]_{mito\text{-}free}$, in both differentiated and undifferentiated HepG2 cells (Fig. 3). However, we found that the steady state levels of $[Ca^{2+}]_{mito\text{-}free}$ in undifferentiated cells were significantly higher, compared to the ones found in differentiated cells (% of fluorescence at time = 0 s, 290 ± 20 vs. 190 ± 10, $p < 0.001$).

2.3. Effect of the enzymatic depletion of polyP on mitochondrial $[Ca^{2+}]_{mito\text{-}free}$

To further confirm that the effects of $[Ca^{2+}]_{mito\text{-}free}$ are likely related to the levels of polyP in mitochondria, we expressed the mitochondrially-targeted GPF-tagged polyphosphatase (MitoPPX) enzyme and measured $[Ca^{2+}]_{mito\text{-}free}$ in the cells. This enzyme expression leads to the depletion of the mitochondrial pool of polyP.

After transfecting HepG2 undifferentiated cells with MitoPPX, we loaded the cells with Rhod-2 and we conducted calcium live measurements, as described in the previous section. The basal levels of $[Ca^{2+}]_{mito\text{-}free}$ inside the mitochondria were the same in both transfected and untransfected cells. Following the addition of ionomycin, the increase in the mitochondrial $[Ca^{2+}]_{mito\text{-}free}$ was significantly higher in the cells that did not express mitoPPX enzyme, compared to the transfected cells (% of fluorescence at time = 0 s, 330 ± 30 vs. 180 ± 20, $p < 0.001$) (Fig. 4). Interestingly, when we tried to repeat the same experiment using differentiated HepG2 cells, the expression of mitoPPX caused dramatic

cell damage. Specifically, cells expressing mitoPPX (identified by GFP fluorescence) became shrunk and rounded. These observations suggest that although the basal levels of polyP in the mitochondria of differentiated cells appears to be lower comparing to undifferentiated cells, some amount of polyP is required for differentiated cells, in order to survive. Interestingly, a similar pattern of polyP distribution and toxic effect of mitoPPX expression was observed in differentiated SH-SY5Y neuroblastoma cells. Similarly to HepG2 cells, almost no signal was detected in the cytoplasmic region of the differentiated SH-SY5Y cells, while significant amounts of polyP were present in nuclei and mitochondria (Supplementary Fig. 5A). The expression of mitoPPX led to similar cell damage that the one observed in the case of the differentiated HepG2 cells.

2.4. Effect of spermine in $[Ca^{2+}]_{mito\text{-}free}$ in HepG2

Next, we attempted to investigate the impact of the polyP inhibition in $[Ca^{2+}]_{mito\text{-}free}$ by using spermine, a drug which can bind polyP with high affinity [45]. Spermine is a polyamine involved in the cellular metabolism and found in all the eukaryotic cells [46]. In addition to its polyP-biding capability, this compound has a wide-spectrum of effects, including anti-oxidant action [47] and modulation of proliferation [48] and differentiation [49] processes. Moreover, spermine can act as a calcium ionophore, inducing physiological calcium signal by itself.

Changes in $[Ca^{2+}]_{mito\text{-}free}$ inside mitochondria were monitored in live cells by using the fluorescence probe Rhod-2 AM, similarly to what we did before in the case of the ionomycin experiments. The response of differentiated and undifferentiated HepG2 cells to spermine was very similar, compared to the one observed after the perfusion with ionomycin. In fact, it appeared a lower increase in $[Ca^{2+}]_{mito\text{-}free}$ in differentiated cells (% of fluorescence at time = 0 s, 290 ± 20 vs. 120 ± 10, $p < 0.001$) (Supplementary Fig. 4A, C). This result was despite the fact that cytoplasmic response to spermine was very similar in both cell types (% of fluorescence at time = 0 s, 198 ± 18 vs. 180 ± 10) (Supplementary Fig. 4B, D). However, taking into account the multiple possible effects of spermine, it is difficult to conclude whether the observed effects are related to the interactions between polyP and spermine or to some other action of the compound.

The addition of ionomycin in the presence of spermine caused a sharp increase in calcium concentrations, in both mitochondria and cytoplasm, which was followed by a marked decrease (Supplementary Fig. 4A, B). This decrease was likely caused by the permeabilization of the mitochondrial membrane and the consequent cell death process, as evidenced by the positive staining of the cells with propidium iodide and by the MTT cell viability assay (Supplementary Fig. 4E). Interestingly, undifferentiated cells demonstrated a slightly lower degree of cell death. This lesser toxic effect of spermine is unlikely due to its bind to polyP. Indeed, previous experiments with the enzymatic removal of polyP from HepG2 cells showed that these cells were protected from ionomycin-induced death, presumably by inhibiting the permeability transition pore [30]. Moreover, in the literature, we found that spermine was not able to inhibit low-conductance calcium-induced permeability transition pore [50].

Taking into account the various effects of spermine and the fact that addition of ionomycin leads to cell permeabilization, it is difficult to establish whether the observed data reflects polyP-spermine interactions or is caused by other mechanisms of action of spermine.

3. Discussion

Here we present experimental evidence that polyP is involved in the regulation of the $[Ca^{2+}]_{mito\text{-}free}$. We found that, under conditions of calcium overload, the levels of $[Ca^{2+}]_{mito\text{-}free}$ are lower when polyP is not present or reduced. We hypothesize that this effect of polyP is linked to its ability to regulate phosphate-calcium interactions.

3.1. Is alkaline phosphatase responsible for decreased levels of polyP in differentiated HepG2 cells?

One of the intriguing and novel observations of our work is the significantly reduced levels of polyP in differentiated HepG2 cells. One characteristic feature of HepG2 cells differentiation is the increase in the expression of alkaline phosphatase [36], which is a potent polyP hydrolyzing enzyme [51]. Thus, one of the possibilities is that the decrease in polyP is directly linked to its polyphosphatase activity. However, this is unlikely the case, since alkaline phosphatase is a secreted enzyme and its activity inside the cell is limited. In support of this interpretation, in our experiments, similarly low levels of polyP were observed in differentiated SH-SY5Y cells which, unlike HepG2 cells, do not express alkaline phosphatase. We propose that the different polyP levels are linked to a mechanism not directly related to the alkaline phosphatase enzyme. Interestingly, high levels of polyP have been reported in other cancer cell lines [52]. One of the possibilities is that polyP might contribute towards proliferative cell energy metabolism and/or gene expression. This phenomenon might have critical implications for cancer cells physiology. However, the exact role of polyP in proliferation remains unclear.

Another noteworthy observation obtained from our studies is the essential role played by mitochondrial polyP in differentiated cells. It has been demonstrated before that polyP is key in mitochondrial energy metabolism [28]. Taking into account that differentiated cells are generally more reliant on mitochondrial oxidative phosphorylation as an energy source, it is possible that disruption of the mitochondrial energetic function in these cells has a more profound effect, comparing to undifferentiated cells, which receive significant amounts of energy from glycolysis and are not that dependent on the mitochondrial function.

3.2. What is the potential mechanism of the polyP regulation of $[Ca^{2+}]_{mito\text{-}free}$?

It is established that mitochondria are capable of accumulating large amounts of total calcium and, at the same time, to maintain the levels of $[Ca^{2+}]_{mito\text{-}free}$ at a very narrow range, typically between 1 and 10 μM. This low $[Ca^{2+}]_{mito\text{-}free}$ can be maintained even if the total concentration of mitochondrial calcium reaches levels up to 1 M [9]. As we introduced before, unlike ER, mitochondria do not have any specific calcium binding proteins that could be involved in the calcium buffering process. Thus, it is generally believed that calcium buffering occurs due to its interactions with orthophosphate [review in [53]]. However, the accumulation of high amounts of calcium and orthophosphate is expected to

lead to the irreversible formation of calcium-phosphate precipitates, which are not generally observed in live cells. Indeed, after mitochondrial depolarization, most of the accumulated calcium becomes released from the mitochondria, which clearly indicates a fast dissociation of the calcium-phosphate complexes [54]. This controversial observation leads to the proposal of the existence of other forms of phosphates involved in calcium buffering.

In fact, it is known that condensed phosphates, pyrophosphate and polyphosphate, are potent inhibitors of the calcium-phosphate precipitation in vitro, at concentrations as low as 10^{-7} M [55]. This effect has also been observed in the calcium-carbonate crystals [56]. Although the exact mechanism of this inhibition is not entirely clear, it has been postulated a “poisoning” effect on the calcium-phosphate crystal growing. The inhibitor effect of long-chain polyP on the calcium-phosphate precipitation was much higher than the effect of pyrophosphate, in the context of bone mineralization [57]. Similar data was obtained in models of aortic calcification in rats, induced by vitamin D, where calcification was completely inhibited, while equivalent doses of orthophosphate were ineffective [58]. This inhibitor effect was not exclusive of the polyP, as also organic phosphates (for example ATP), were also able to exert it [59]. However, orthophosphate did not show any inhibiting action [60]. Moreover, it is known that polyP is critical during the process of bone tissue development, where calcium plays a crucial role [40,61,62]. All this data suggest an important role of polyP in the regulation of free calcium. However, this is the first time that a study showing the relationship between polyP and calcium precipitation has been specifically focused on mitochondria. Here we show data concluding that a similar effect of that observed outside the organelle also happens inside, where, according to our data, the concentrations of polyP are much higher and there are not specific proteins to buffer calcium. Specifically, we hypothesize that, inside the mitochondria, polyP is capable of inhibiting calcium-phosphate precipitation, increasing the concentration of mitochondrial free calcium.

This ability of polyP to regulate $[Ca^{2+}]_{mito\text{-}free}$ might potentially have significance not only under conditions of calcium overload; as suggested by previous works which demonstrated the relationship between the levels of polyP, calcium and ROS and the activation of the mitochondrial permeability transition pore, but also in the process of calcium-induced regulation of energy metabolism. Indeed, both polyP and calcium are believed to be involved in the regulation of the mitochondrial energy metabolism [28]. It is interesting to consider the existence of a link between the levels of calcium, polyP and the bioenergetic status of the cell.

While our data suggest the existence of a clear link between the levels of mitochondrial polyP and free calcium under calcium overloading conditions, this study has some limitations, which need to be taken into account. Due to the experimental difficulties, we cannot provide the exact quantification of the mitochondrial polyP and inorganic orthophosphate. However, considering the high potency of PPX enzyme [29], we can suggest that in these cells most of the free polyP has been depleted. We should note that the levels of polyP in mammalian cells are likely very low [26,30] comparing to the levels of orthophosphate and, thus, it is unlikely that polyP hydrolysis will directly cause appreciable changes in the orthophosphate presence inside the cells. Moreover, the data regarding the experiments with spermine is hard to interpret, mainly because of the wide-spectrum effect

of this drug. However, the observed effects of spermine in HepG2 cells suggest the possibility that polyP also contributes towards the regulation of the levels of free calcium in mitochondria, during non-overloading conditions. To properly establish these effects will require more detailed future studies.

In conclusion, we found that decreased mitochondrial polyP leads to the reduced levels of $[Ca^{2+}]_{mito\text{-}free}$ during ionomycin-induced calcium overload. We propose that polyP, which has previously shown an effect on preventing the calcium-phosphate precipitation in other systems, is a previously unrecognized important component of the mitochondrial calcium buffering system.

4. Materials and methods

4.1. Reagents and plasmid

Dulbecco's Modified Eagle medium (DMEM), DMEM:F12, penicillin-streptomycin, fetal bovine serum (FBS) and lipofectamine were purchased from Gibco-Invitrogen (Carlsbad, California, US); polypropylene columns from Qiagen (Venlo, Limburg, The Netherlands); gelatin from BioRad (Hercules, California, US); His60Ni superflow resin from Clontech (Mountain View, California, US); protease inhibitors from Roche (Basel, Switzerland); poly-L-lysine, glucose, ampicillin, luria broth (LB), spermine, isopropyl ß-D-1-thiogalactopyranoside (IPTG), thiazolyl blue tetrazolium Bromide (MTT), propidium iodide, NaCl, $MgCl_2$, KCl, sucrose, digitonin, glycerol, ß-mercaptoethanol, phenylmethanesulfonylfluoride (PMSF), triton X-100, imidazole, ascorbic acid, carbonyl cyanide 4-trifluoromethoxyphenylhydrazone (FCCP), retinoic acid, tris buffered saline (TBS) and dimethyl sulfoxide (DMSO) from Sigma-Aldrich (St. Louis, Missouri, US); MicroBCA Protein Reagent Kit, Restore Western Blot Stripping Buffer and Pierce ECL Plus Substrate Kit from ThermoFisher (Waltham, Massachusetts, US); paraformaldehyde from Electron Microscopy Sciences (Hatfield, Pennsylvania, US); Rhod-2 AM, Fluo-4 AM, tetramethylrhodamine methyl ester (TMRM), Hank's Balanced Salt Solution (HBSS), Hoechst 333,258, HEPES-KOH and Anti-Xpress antibody from LifeTechnologies (Carlsbad, California, US); Peroxidase-conjugated anti-mouse antibody from Promega (Fitchburg, Wisconsin, US); and TOMM20, Alkaline Phosphatase, Actin, Alexa Fluor 488 and Alexa Fluor 555 antibodies and inomycin from Abcam (Cambridge, United Kingdom). DNA construct for PolyP binding domain (PPBD) expression and purification was provided by Dr. Saito.

4.2. Cell culture

HepG2 cells were obtained from the American Type Culture Collection (ATCC) and grown on DMEM, supplemented with 20 units/mL penicillin–streptomycin and 15% (v/v) FBS. SH-SY5Y were also obtained from the ATCC (Manassas, Virginia, US) and grown as reported on [63]. Briefly, they were grown on DMEM:F12, also supplemented with 20 units/mL penicillin–streptomycin and 15% (v/v) FBS. HepG2 cells were differentiated with 2% DMSO for 15 days while SH-SY5Y were differentiated with 10 mM retinoic acid for 6 days. All cell types were grown in a humidified cell culture incubator, under 5% CO_2 atmosphere, at 37 °C.

4.3. Western blotting

Western blotting was performed as previously described [64], but using an anti-alkaline phosphatase antibody. Briefly, cells were washed with cold PBS and lysed for 5 min in 30 μL of cold lysis buffer, containing 80 mM KCl, 250 mM sucrose, 500 μg/mL digitonin, protease inhibitor cocktail and 0.1 mM PMSF in PBS. Cells lysates were centrifuged for 5 min at 10,000 ×g. Protein concentration quantification was performed spectrophotometrically with the MicroBCA kit, following the manufacturer specifications. 30 μg of protein was loaded onto 10% Mini-PROTEAN TGX Precast Gels (BioRad, Hercules, California, US). After electrophoresis, proteins were transferred to Immun-Blot PVDF Membrane for Protein Blotting, (BioRad, Hercules, California, US). Non-specific protein binding was blocked with Super-Block Blocking Buffer in TBS (ThermoFisher, Waltham, Massachusetts, US) for 1 h. The membranes were then incubated with anti-alkaline phosphatase antibody (1:1000 dilution) overnight at 4 °C, under agitation. After washing the membranes with Super-Block Blocking Buffer on TBS, they were incubated with a secondary antibody (1:5000 dilution). Then, several washes were made and the signal was detected using the Pierce ECL Plus Substrate Kit, following the indications of the manufacturer. After re-blotting the membranes with Restore Western Blot Stripping Buffer, following the indications of the manufacturer, the process was repeated, using an anti-actin antibody (1:1000 dilution).

4.4. PPBD amplification and purification

PPBD was amplified on BL21 cells (Life Technologies, Carlsbad, California, US) following the manufacture's protocol. Then, it was purified. For that, 200 μL of the transformation mixture were added to 30 mL of LB, containing 100 μg/mL ampicillin and 20 mM glucose and incubated overnight at 37 °C, with 255 rpm shaking. The day after, 100 μL of the overnight culture was added to 100 mL of LB, containing ampicillin 100 μg/mL and 40 mM glucose and incubated at 255 rpm and 37 °C. After 3 h, 1 mM of fresh-prepared IPTG was added to the mixture and the incubation continued, under the same conditions, for 2.5 additional hours. Cells were then pelleted and frozen at −80 °C, overnight. The day after, cells were thrown on ice, resuspended on 20 mL of "Buffer 1" (10 mM HEPES-KOH, 0.1 M NaCl, 5 mM $MgCl_2$, 10% glycerol, 2 mM ß-mercaptoethanol, 1 mM PMSF and protease inhibitors, pH = 7.6) and sonicated 4 times for 1 min, waiting 1 min between each sonication cycle. After that, 0.1% Triton X-100 was added to the cell lysate and it was incubated at room temperature for 30 min, at 255 rpm shaking. Half an hour later, cells were centrifuged at 20,000 ×g for 10, at 4 °C. Simultaneously, polypropylene columns were loaded with His60Ni superflow resin and equilibrated with "Buffer 2" (10 mM HEPES-KOH, 0.5 M NaCl, 5 mM $MgCl_2$, 10% glycerol, 0.1% Triton X-100, 2 mM ß-mercaptoethanol, pH = 7.6) supplemented with 20 mM imidazole. The centrifugation supernatant was filtered through 22 μm filters and 20 mM imidazole was added just before the 30 min incubation at 4 °C. After that, the lysate was added to the columns, and let to pass throw by gravity. Columns were washed twice with buffer 2 and twice again with buffer 2 supplemented with 50 mM imidazole. PPBD was then eluted with 500 μL of buffer 2, containing 350 mM imidazole. Elution was repeated six times, using new tubes each time, to ensure the complete elution of the PPBD. Protein was quantified and a gel was run, in order to check the presence of the PPBD.

4.5. Immunocytochemistry and co-localization measurement

Cells were plated on 15 mm optical borosilicate poly-L-lysine-coated sterile cover glasses (ThermoFisher, Waltham, Massachusetts, US) at a 70% confluence. 24 h later, cells were fixed on 4% paraformaldehyde and washed once for 5 min with PBS and twice for 5 min with TBS (pH = 8.3). Cells were then permeabilized with 0.1% Triton X-100 and 0.5 mM $MgCl_2$ on TBS (pH = 8.3) for 2 min at room temperature. After that, cells were washed two times with TBS (pH = 8.3) and blocked with 3% gelatin and 0.5 mM $MgCl_2$ on TBS for an hour, at 30 °C, under 30 rpm agitation. Then, this solution was replaced by a new one, containing 20 μg/mL of PPBD in blocking buffer for an hour, at the same conditions. Cells were then washed twice for 5 min with TBS (pH = 8.3), incubated with 2 μg/mL of mouse Anti-Xpress antibody in blocking solution for an hour at 30 rpm, and washed once with 0.05% Triton X-100 on TBS and twice with TBS, (pH = 8.3). Next, rabbit monoclonal TOMM20 antibody was added (1:200 dilution), to cells in blocking solution and at the same conditions as PPBD, and the washes were repeated. Finally, Alexa Fluor 488 goat anti-mouse and Alexa Fluor 555 donkey anti-rabbit antibodies were added together, at a 1:200 dilution, also in blocking solution, for an hour, at 30 °C and 30 rpm agitation. Then, cells were washed once with Triton 0.01% in TBS, (pH = 8.3), twice with TBS and once with water. The cell images were obtained using a Zeiss-LSM710 confocal microscope (63× oil-immersion objective) with appropriate fluorescent filters. For the co-localization measurement, micrographs were analyzed by using the Colocalization plugin from ImageJ. We considered co-localization in those areas where 30% or more of the points were present in both channels.

4.6. Mitochondrial and cytoplasmic calcium assay

Cells were plated on 25 mm optical borosilicate poly-L-lysine-coated sterile cover glasses, (ThermoFisher, Waltham, Massachusetts, US) at a 70% confluence. 24 h later, cells were loaded with either 5 μM Rhod-2 AM or 2.5 μM Fluo-4 AM on HBSS for 45 min. Then, cells were washed twice with HBSS and incubated for another additional 15 min on fresh HBSS, without Rhod-2 AM or Fluo-4 AM. After that, HBSS was replaced again by fresh HBSS, glasses were mounted on microscopy chambers and experiments were conducted. Stock solutions of spermine (0.01 M) and ionomycin (5 mM) were prepared on DMSO. For treatments, drugs were diluted on HBSS to the working concentration, that is, 0.1 mM and 5 μM, respectively. Cells were imaged every 5s at a 20 × magnification, using a Nikon fluorescent microscope (Chiyoda, Tokyo, Japan). Drugs were added by complete bath perfusion at fixed times, to secure their homogeneous distribution as well as the reproducibility of the experiments. Images were processed using NIS-Elements and ImageJ software. For some time-based fluorescence assays, fluorescent signal at the beginning of the experiment was normalized to 100% and fluorescence was expressed as a percentage change. We used Rhod-2 AM, a non-ratiometric calcium-sensitive mitochondrial probe, because our main interest on this manuscript was to visualize and compare relative levels of $[Ca^{2+}]_{mito\text{-}free}$ between different cell types. Since ratiometric Fura-2 is not mitochondrial specif-ic, we did not use it in this work. In order to try to avoid the variations in the data due to experimental differences between the glasses, we kept all the experimental procedures as constant as possible and we stan-dardized all the values with the internal controls from each experiment. The representative data from individual experiments expressed in absolute

values of fluorescence (arbitrary units — AU) are shown in Supplementary Fig. 2A and B, for the experiments with differentiated and undifferentiated cells and for the ones with transfected and untransfected undifferentiated HepG2 cells, respectively.

4.7. Cell death assay

For the cell death assay, HepG2 cells were seeded on 12-wells tissue-cultured treated plastic plates, at a confluence of 5×10^5 viable cells per mL of medium. In the case of the differentiated cell cultures, HepG2 cells were plated seven days prior running the experiments and the differentiation was finished on the 12-wells plates. On the day of the experiment, cells were placed into HBSS and treated with the different drugs, prepared as explained in the previous paragraph. Drugs were added to the cultures, in the presence of 10 μg/mL propidium iodide and 10 μg/mL Hoechst 33258. After running a cell viability assay (data not shown), we determined that 3 was the proper time to perform our experiments. Thus, 3 h after adding the drugs to our cultures, cells were visualized by using a 20× objective on a Nikon fluorescence microscope (Chiyoda, Tokyo, Japan) and five pictures per well were taken. Every condition was repeated at least three times, in duplicate. Images were analyzed by using the image-based tool for counting nuclei (ITCN) from ImageJ. MTT cell viability assay was performed following the standard protocol. Briefly, cells were plated on 96-wells plates. The day after, a solution containing 0.05% w/v of MTT on fresh medium was prepared. The medium from the cells was replaced by 150 μL per well of the medium containing MTT and the plate was incubated for 2 h at 37 °C. After that, the medium containing MTT was replaced by 150 μL of DMSO per well. The place was shacked and an spectrophotometrical measurement at 540 nm (for life cells) and at 685 nm (for background) was performed.

4.8. Cell DNA transfection

For DNA transfection cells were plated on 25 mm optical borosilicate poly-L-lysine-coated sterile cover glasses (ThermoFisher, Waltham, Massachusetts, US) at a 70% confluence. Transfection was performed 24 h later using Lipofectamine, as previously reported, [64]. Briefly, cells were transfected with 3.2 μg/mL of DNA plasmid encoding MitoPPX, in culture medium without FBS or antibiotic. After 4 h of incubation, the transfection mixture was replaced by fresh complete medium and the experiments were conducted 24 h after, in order to allow protein expression.

4.9. Statistical analysis

Statistical significance of differences between groups was determined by Student’s test or two-tailed Student’s test. The level of statistical significance was set at $p < 0.01$. For the statistical analysis and the graphical representation Origins Lab software was used.

Supplementary Material

Refer to Web version on PubMed Central for supplementary material.

Acknowledgments

We acknowledge Dr. M. Saito and Dr. K. Saito, from the Department of Environmental Chemistry, National Institute for Agro-Environmental Sciences, Tsukuba, Ibaraki, Japan for providing us with the PPBD that they constructed. This research was supported by the National Institutes of Health through grant R01GM098052 to E.Z. and by NYU University Research Challenge Fund (R4697) grant to E.P.

References

[1]. Berridge MJ, Lipp P, Bootman MD, The versatility and universality of calcium signalling, Nat. Rev. Mol. Cell Biol 1 (2000) 11–21. [PubMed: 11413485]

[2]. Carafoli E, Santella L, Branca D, Brini M, Generation, control, and processing of cellular calcium signals, Crit. Rev. Biochem. Mol. Biol 36 (2001) 107–260. [PubMed: 11370791]

[3]. Orrenius S, Zhivotovsky B, Nicotera P, Regulation of cell death: the calcium-apoptosis link, Nat. Rev. Mol. Cell Biol 4 (2003) 552–565. [PubMed: 12838338]

[4]. Syntichaki P, Tavernarakis N, The biochemistry of neuronal necrosis: rogue biology? Nat. Rev. Neurosci 4 (2003) 672–684. [PubMed: 12894242]

[5]. Yanez M, Gil-Longo J, Campos-Toimil M, Calcium binding proteins, Adv. Exp. Med. Biol 740 (2012) 461–482. [PubMed: 22453954]

[6]. Rossi CS, Lehninger AL, Stoichiometry of respiratory stimulation, accumulation of Ca^{++} and phosphate, and oxidative phosphorylation in rat liver mitochondria, J. Biol. Chem 239 (1964) 3971–3980. [PubMed: 14257633]

[7]. Lehninger AL, Role of phosphate and other proton-donating anions in respiration-coupled transport of Ca^{2+} by mitochondria, Proc. Natl. Acad. Sci. U. S. A 71 (1974) 1520–1524. [PubMed: 4364542]

[8]. Wei AC, Liu T, O'Rourke B, Dual effect of phosphate transport on mitochondrial Ca^{2+} dynamics, J. Biol. Chem (2015).

[9]. Chalmers S, Nicholls DG, The relationship between free and total calcium concentrations in the matrix of liver and brain mitochondria, J. Biol. Chem 278 (2003) 19062–19070. [PubMed: 12660243]

[10]. Bazil JN, Blomeyer CA, Pradhan RK, Camara AK, Dash RK, Modeling the calcium sequestration system in isolated guinea pig cardiac mitochondria, J. Bioenerg. Biomembr 45 (2013) 177–188. [PubMed: 23180139]

[11]. Blomeyer CA, Bazil JN, Stowe DF, Pradhan RK, Dash RK, Camara AK, Dynamic buffering of mitochondrial Ca^{2+} during Ca^{2+} uptake and Na^{+}-induced Ca^{2+} release, J. Bioenerg. Biomembr 45 (2013) 189–202. [PubMed: 23225099]

[12]. Solesio ME, Saez-Atienzar S, Jordan J, Galindo MF, Characterization of mitophagy in the 6-hydoxydopamine Parkinson's disease model, Toxicol. Sci 129 (2012) 411–420. [PubMed: 22821850]

[13]. Solesio ME, Saez-Atienzar S, Jordan J, Galindo MF, 3-Nitropropionic acid induces autophagy by forming mitochondrial permeability transition pores rather than activating the mitochondrial fission pathway, Br. J. Pharmacol 168 (2013) 63–75. [PubMed: 22509855]

[14]. Fossati S, Giannoni P, Solesio ME, et al., The carbonic anhydrase inhibitor methazolamide prevents amyloid beta-induced mitochondrial dysfunction and caspase activation protecting neuronal and glial cells in vitro and in the mouse brain, Neurobiol. Dis 86 (2015) 29–40. [PubMed: 26581638]

[15]. Lamb R, Ozsvari B, Lisanti CL, et al., Antibiotics that target mitochondria effectively eradicate cancer stem cells, across multiple tumor types: treating cancer like an infectious disease, Oncotarget 6 (2015) 4569–4584. [PubMed: 25625193]

[16]. Scatena R, Mitochondria and cancer: a growing role in apoptosis, cancer cell metabolism and dedifferentiation, Adv. Exp. Med. Biol 942 (2012) 287–308. [PubMed: 22399428]

[17]. Lemieux H, Hoppel CL, Mitochondria in the human heart, J. Bioenerg. Biomembr 41 (2009) 99–106. [PubMed: 19353253]

[18]. Walters AM, Porter GA Jr., Brookes PS, Mitochondria as a drug target in ischemic heart disease and cardiomyopathy, Circ. Res 111 (2012) 1222–1236. [PubMed: 23065345]

[19]. Stotz SC, Scott LO, Drummond-Main C, et al., Inorganic polyphosphate regulates neuronal excitability through modulation of voltage-gated channels, Mol. Brain 7 (2014) 42. [PubMed: 24886461]

[20]. Holmstrom KM, Marina N, Baev AY, Wood NW, Gourine AV, Abramov AY, Signalling properties of inorganic polyphosphate in the mammalian brain, Nat. Commun 4 (2013) 1362. [PubMed: 23322050]

[21]. Morrissey JH, Choi SH, Smith SA, Polyphosphate: an ancient molecule that links platelets, coagulation, and inflammation, Blood 119 (2012) 5972–5979. [PubMed: 22517894]

[22]. Seidlmayer LK, Juettner VV, Kettlewell S, Pavlov EV, Blatter LA, Dedkova EN, Distinct mPTP activation mechanisms in ischaemia–reperfusion: contributions of Ca^{2+}, ROS, pH, and inorganic polyphosphate, Cardiovasc. Res 106 (2015) 237–248. [PubMed: 25742913]

[23]. Rao NN, Gomez-Garcia MR, Kornberg A, Inorganic polyphosphate: essential for growth and survival, Annu. Rev. Biochem 78 (2009) 605–647. [PubMed: 19344251]

[24]. Leyhausen G, Lorenz B, Zhu H, et al., Inorganic polyphosphate in human osteoblast-like cells, J. Bone Miner. Res 13 (1998) 803–812. [PubMed: 9610744]

[25]. Ruiz FA, Lea CR, Oldfield E, Docampo R, Human platelet dense granules contain polyphosphate and are similar to acidocalcisomes of bacteria and unicellular eukaryotes, J. Biol. Chem 279 (2004) 44250–44257. [PubMed: 15308650]

[26]. Kumble KD, Kornberg A, Inorganic polyphosphate in mammalian cells and tissues, J. Biol. Chem 270 (1995) 5818–5822. [PubMed: 7890711]

[27]. Schroder HC, Kurz L, Muller WE, Lorenz B, Polyphosphate in bone, Biochemistry (Mosc) 65 (2000) 296–303. [PubMed: 10739471]

[28]. Pavlov E, Aschar-Sobbi R, Campanella M, Turner RJ, Gomez-Garcia MR, Abramov AY, Inorganic polyphosphate and energy metabolism in mammalian cells, J. Biol. Chem 285 (2010) 9420–9428. [PubMed: 20124409]

[29]. Abramov AY, Fraley C, Diao CT, et al., Targeted polyphosphatase expression alters mitochondrial metabolism and inhibits calcium-dependent cell death, Proc. Natl. Acad. Sci. U. S. A 104 (2007) 18091–18096. [PubMed: 17986607]

[30]. Seidlmayer LK, Gomez-Garcia MR, Blatter LA, Pavlov E, Dedkova EN, Inorganic polyphosphate is a potent activator of the mitochondrial permeability transition pore in cardiac myocytes, J. Gen. Physiol 139 (2012) 321–331. [PubMed: 22547663]

[31]. Seidlmayer LK, Blatter LA, Pavlov E, Dedkova EN, Inorganic polyphosphate–an unusual suspect of the mitochondrial permeability transition mystery, Channels (Austin) 6 (2012) 463–467. [PubMed: 22990682]

[32]. Solesio ME, Elustondo PA, Zakharian E, Pavlov EV, Inorganic polyphosphate (polyP) as an activator and structural component of the mitochondrial permeability transition pore, Biochem. Soc. Trans 44 (2016) 7–12. [PubMed: 26862181]

[33]. Smithen M, Elustondo PA, Winkfein R, Zakharian E, Abramov AY, Pavlov E, Role of polyhydroxybutyrate in mitochondrial calcium uptake, Cell Calcium 54 (2013) 86–94. [PubMed: 23702223]

[34]. Caro AA, Cederbaum AI, Role of calcium and calcium-activated proteases in CYP2E1-dependent toxicity in HEPG2 cells, J. Biol. Chem 277 (2002) 104–113. [PubMed: 11689564]

[35]. Leite MF, Thrower EC, Echevarria W, et al., Nuclear and cytosolic calcium are regulated independently, Proc. Natl. Acad. Sci. U. S. A 100 (2003) 2975–2980. [PubMed: 12606721]

[36]. Guo L, Song L, Wang Z, Zhao W, Mao W, Yin M, Panaxydol inhibits the proliferation and induces the differentiation of human hepatocarcinoma cell line HepG2, Chem. Biol. Interact 181 (2009) 138–143. [PubMed: 19450571]

[37]. Kim EE, Wyckoff HW, Reaction mechanism of alkaline phosphatase based on crystal structures. Two-metal ion catalysis, J. Mol. Biol 218 (1991) 449–464. [PubMed: 2010919]

[38]. Wanner BL, Latterell P, Mutants affected in alkaline phosphatase, expression: evidence for multiple positive regulators of the phosphate regulon in Escherichia coli, Genetics 96 (1980) 353–366. [PubMed: 7021308]

[39]. Lorenz B, Schroder HC, Mammalian intestinal alkaline phosphatase acts as highly active exopolyphosphatase, Biochim. Biophys. Acta 1547 (2001) 254–261. [PubMed: 11410281]

[40]. Omelon S, Georgiou J, Variola F, Dean MN, Colocation and role of polyphosphates and alkaline phosphatase in apatite biomineralization of elasmobranch tesserae, Acta Biomater 10 (2014) 3899–3910. [PubMed: 24948547]

[41]. Pike AF, Kramer NI, Blaauboer BJ, Seinen W, Brands R, A novel hypothesis for an alkaline phosphatase 'rescue' mechanism in the hepatic acute phase immune response, Biochim. Biophys. Acta 2013 (1832) 2044–2056.

[42]. Saito K, Ohtomo R, Kuga-Uetake Y, Aono T, Saito M, Direct labeling of polyphosphate at the ultrastructural level in Saccharomyces cerevisiae by using the affinity of the polyphosphate binding domain of Escherichia coli exopolyphosphatase, Appl. Environ. Microbiol 71 (2005) 5692–5701. [PubMed: 16204477]

[43]. Liu C, Hermann TE, Characterization of ionomycin as a calcium ionophore, J. Biol. Chem 253 (1978) 5892–5894. [PubMed: 28319]

[44]. Abramov AY, Duchen MR, Actions of ionomycin, 4-BrA23187 and a novel electrogenic Ca^{2+} ionophore on mitochondria in intact cells, Cell Calcium 33 (2003) 101–112. [PubMed: 12531186]

[45]. Smith SA, Choi SH, Collins JN, Travers RJ, Cooley BC, Morrissey JH, Inhibition of polyphosphate as a novel strategy for preventing thrombosis and inflammation, Blood 120 (2012) 5103–5110. [PubMed: 22968458]

[46]. Heby O, Persson L, Molecular genetics of polyamine synthesis in eukaryotic cells, Trends Biochem. Sci 15 (1990) 153–158. [PubMed: 2187296]

[47]. Mozdzan M, Szemraj J, Rysz J, Stolarek RA, Nowak D, Anti-oxidant activity of spermine and spermidine re-evaluated with oxidizing systems involving iron and copper ions, Int. J. Biochem. Cell Biol 38 (2006) 69–81. [PubMed: 16107320]

[48]. Mandal S, Mandal A, Johansson HE, Orjalo AV, Park MH, Depletion of cellular polyamines, spermidine and spermine, causes a total arrest in translation and growth in mammalian cells, Proc. Natl. Acad. Sci. U. S. A 110 (2013) 2169–2174. [PubMed: 23345430]

[49]. Quemener V, Blanchard Y, Lescoat D, Havouis R, Moulinoux JP, Depletion in nuclear spermine during human spermatogenesis, a natural process of cell differentiation, Am. J. Phys 263 (1992) C343–C347.

[50]. Elustondo PA, Negoda A, Kane CL, Kane DA, Pavlov EV, Spermine selectively inhibits high-conductance, but not low-conductance calcium-induced permeability transition pore, Biochim. Biophys. Acta 2015 (1847) 231–240.

[51]. Tammenkoski M, Koivula K, Cusanelli E, et al., Human metastasis regulator protein H-prune is a short-chain exopolyphosphatase, Biochemistry 47 (2008) 9707–9713. [PubMed: 18700747]

[52]. Demirkhanyan L, Elustondo P, Pavlov E, Zakharian E, Role of polyphosphate in cancer cell proliferation, Biophys. J 106 (2014) 753a.

[53]. Nicholls DG, Chalmers S, The integration of mitochondrial calcium transport and storage, J. Bioenerg. Biomembr 36 (2004) 277–281. [PubMed: 15377857]

[54]. Bernardi P, Mitochondrial transport of cations: channels, exchangers, and permeability transition, Physiol. Rev 79 (1999) 1127–1155. [PubMed: 10508231]

[55]. Fleisch H, Bisaz S, Mechanism of calcification: inhibitory role of pyrophosphate, Nature 195 (1962) 911.

[56]. Arai T, Kuwahara S, Studies on the influence of minute amounts of fatty acids in bacteriological culture media on bacterial growth (I). Growth-accelerating action of trace amounts of fatty acids in vitamin-free casin acid-hydrolysate on Streptococcus hemolyticus strain S-8, Jpn. J. Microbiol 5 (1961) 327–335. [PubMed: 14013520]

[57]. Fleisch H, Straumann F, Schenk R, Bisaz S, Allgower M, Effect of condensed phosphates on calcification of chick embryo femurs in tissue culture, Am. J. Phys 211 (1966) 821–825.

[58]. Fleisch H, Schibler D, Maerki J, Frossard I, Inhibition of aortic calcification by means of pyrophosphate and polyphosphates, Nature 207 (1965) 1300–1301.

[59]. Fleish H, Neuman WF, Mechanisms of calcification: role of collagen, polyphosphates, and phosphatase, Am. J. Phys 200 (1961) 1296–1300.

[60]. Fleisch H, Bisaz S, Isolation from urine of pyrophosphate, a calcification inhibitor, Am. J. Phys 203 (1962) 671–675.

[61]. Omelon S, Georgiou J, Henneman ZJ, et al., Control of vertebrate skeletal mineralization by polyphosphates, PLoS One 4 (2009), e5634. [PubMed: 19492083]

[62]. Omelon SJ, Grynpas MD, Relationships between polyphosphate chemistry, biochemistry and apatite biomineralization, Chem. Rev 108 (2008) 4694–4715. [PubMed: 18975924]

[63]. Perez-Alvarez S, Iglesias-Guimarais V, Solesio ME, et al., Methadone induces CAD degradation and AIF-mediated necrotic-like cell death in neuroblastoma cells, Pharmacol. Res 63 (2011) 352–360. [PubMed: 21145398]

[64]. Solesio ME, Prime TA, Logan A, et al., The mitochondria-targeted anti-oxidant MitoQ reduces aspects of mitochondrial fission in the 6-OHDA cell model of Parkinson's disease, Biochim. Biophys. Acta 2013 (1832) 174–182.

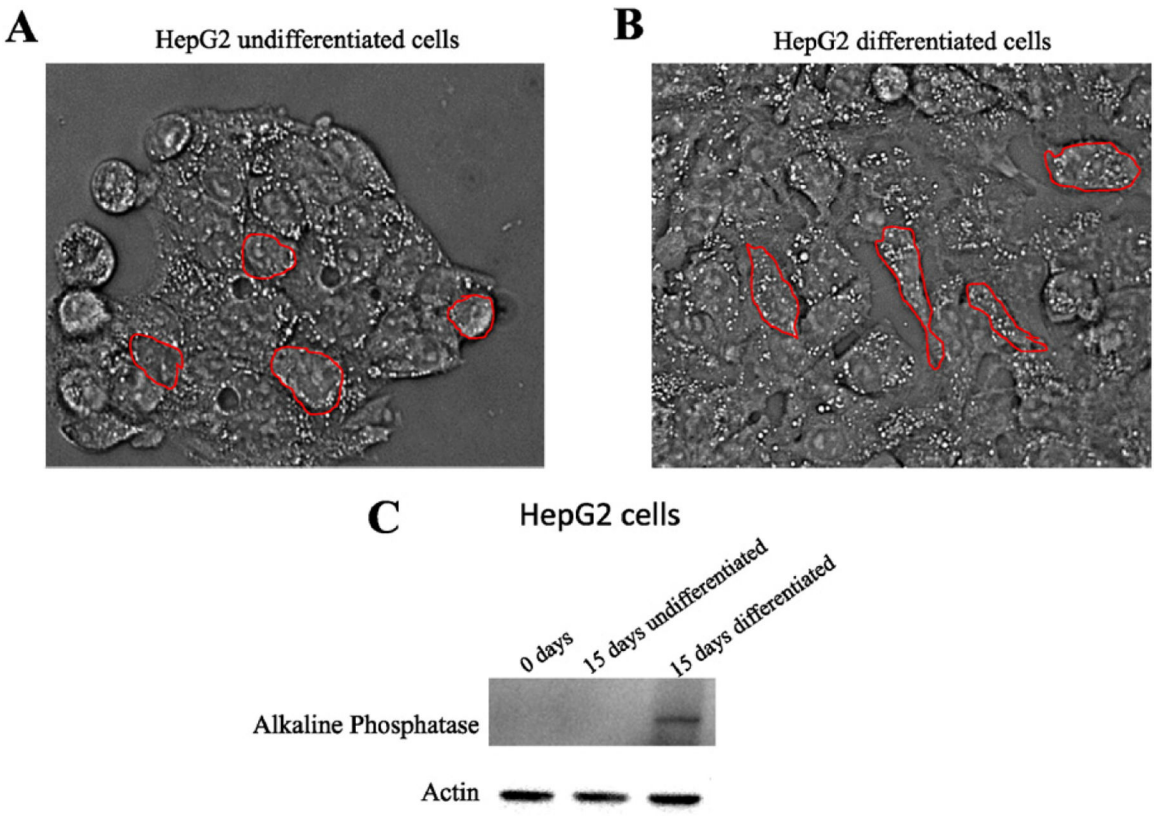

Fig. 1.

Morphological differences between differentiated and undifferentiated HepG2 cells. A. Undifferentiated cells grow in clusters and have round shape. Once these aggregations were formed, cells were not able to grow normally again. B. Differentiated cells are less aggregated, showing a more elongated morphology, compared to the undifferentiated ones. When HepG2 cells were differentiated, they were able to reach 100% of confluence. C. Western Blot showing the different levels of alkaline phosphatase on undifferentiated and differentiated HepG2. Actin was used as loading control.

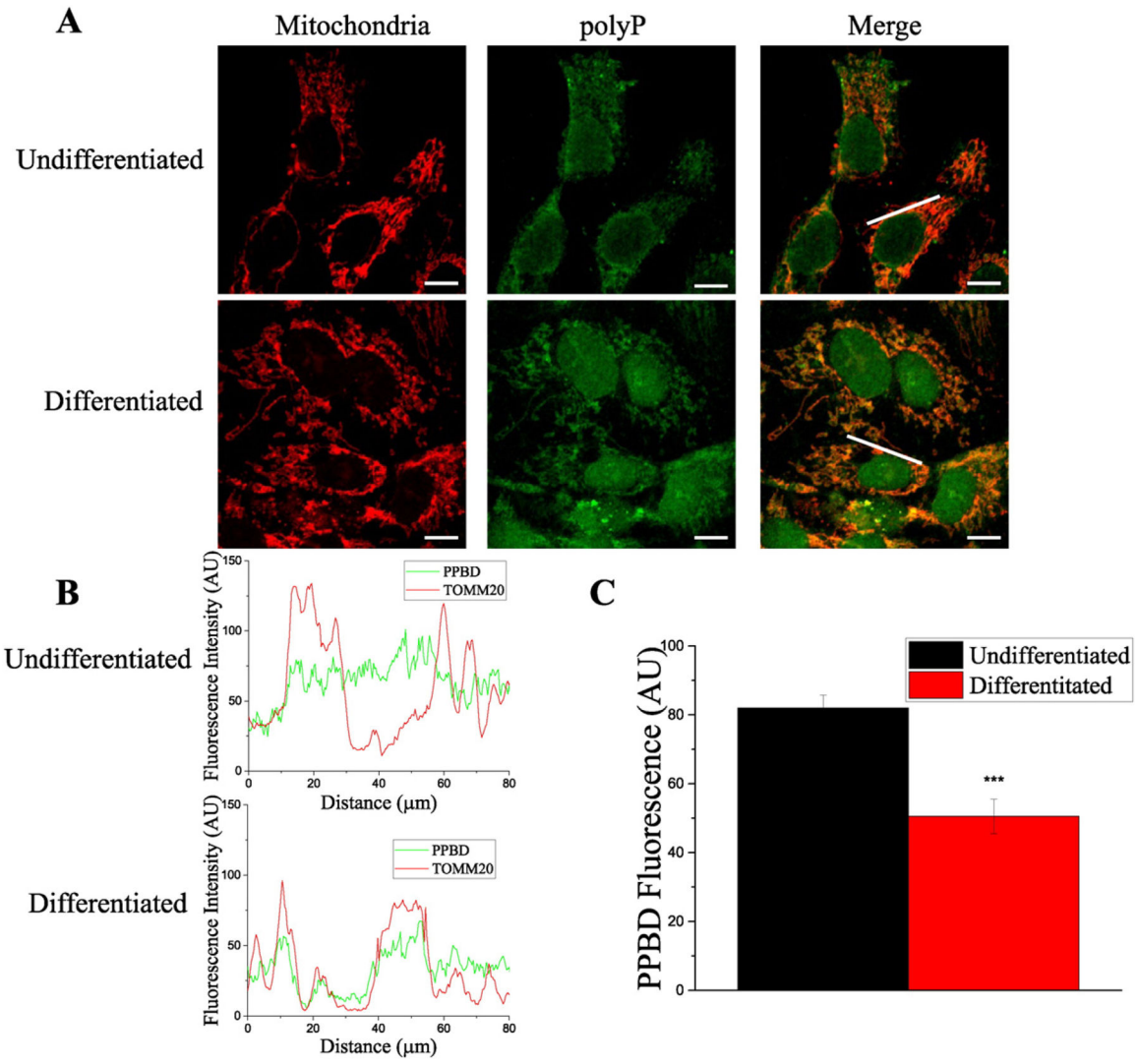

Fig. 2.

PolyP presence and distribution on HepG2 undifferentiated and differentiated cells. A. After the immunocytochemistry assay, confocal images of representative fields were taken. PolyP (visualized with the PPBD assay) is labeled in green and mitochondria are labeled in red (visualized with TOMM20 antibodies). B. Colocalization plots showing fluorescence intensity profiles along the white lines showed on the “Merge” images of undifferentiated and differentiated cells, in upper and lower plots, respectively. Note that after HepG2 differentiation, polyP was not present in cytoplasm, and reduced in mitochondria. C. Histogram showing PPBD fluorescence in both undifferentiated and differentiated HepG2 cells, along the white lines showed on the “merge” images. Scale bar = 50 μm. Data in histograms are mean ± SEM of ten ROIs from four independent experiments. Student’s test: ***$p < 0.001$.

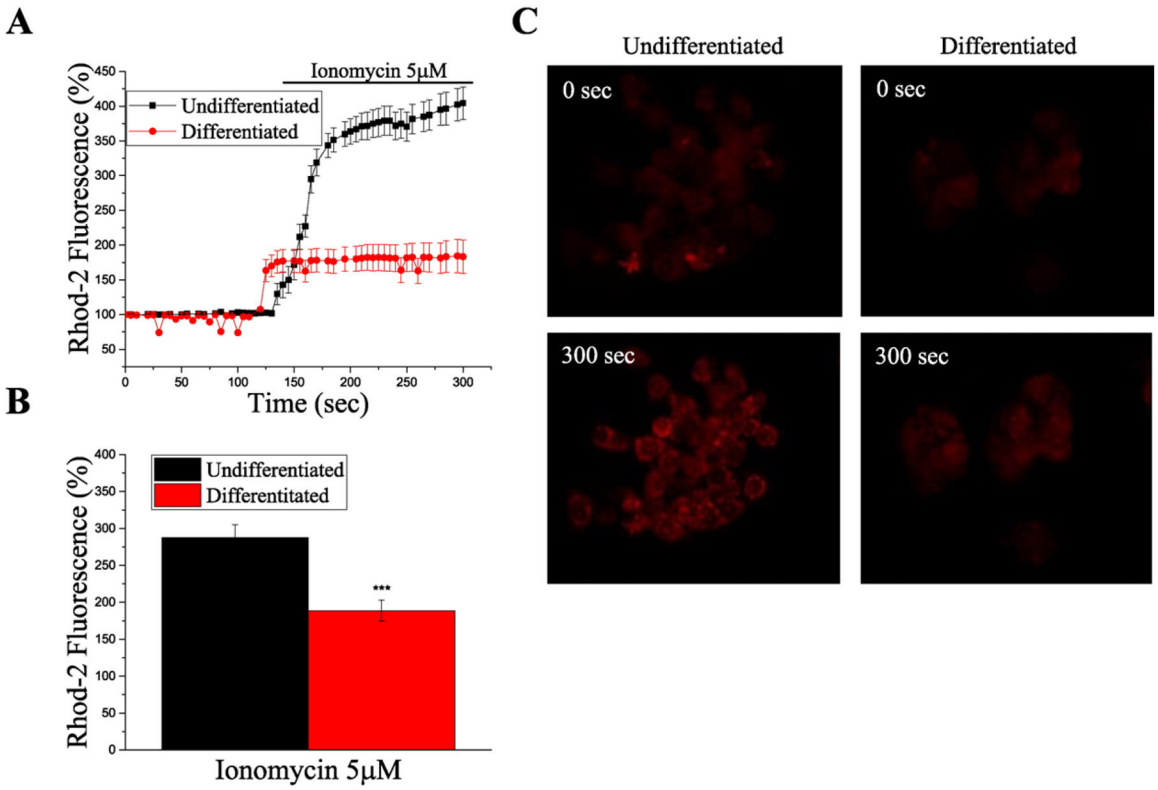

Fig. 3.

[Ca^{+2}]mito-free is reduced in differentiated HepG2 cells. A. Graph showing real-time measurement of [Ca^{+2}]mito-free using Rhod-2 fluorescent probe. Note the significantly lower [Ca^{+2}]mito-free in differentiated cells, in the presence of ionomycin. Data is shown as mean ± SEM of, at least, ten different cells from the same field. B. Histogram showing Rhod-2 fluorescence after 180 s of recording, (50 s after the addition of ionomycin), in undifferentiated and differentiated HepG2 cells. Data shown as mean ± SEM of, at least, ten different cells per experiment from, at least, three independent experiments. Student's test: ***$p < 0.001$. C. Representative images of the Rhod-2 fluorescence in undifferentiated and differentiated HepG2 cells, corresponding to the graph shown on panel A.

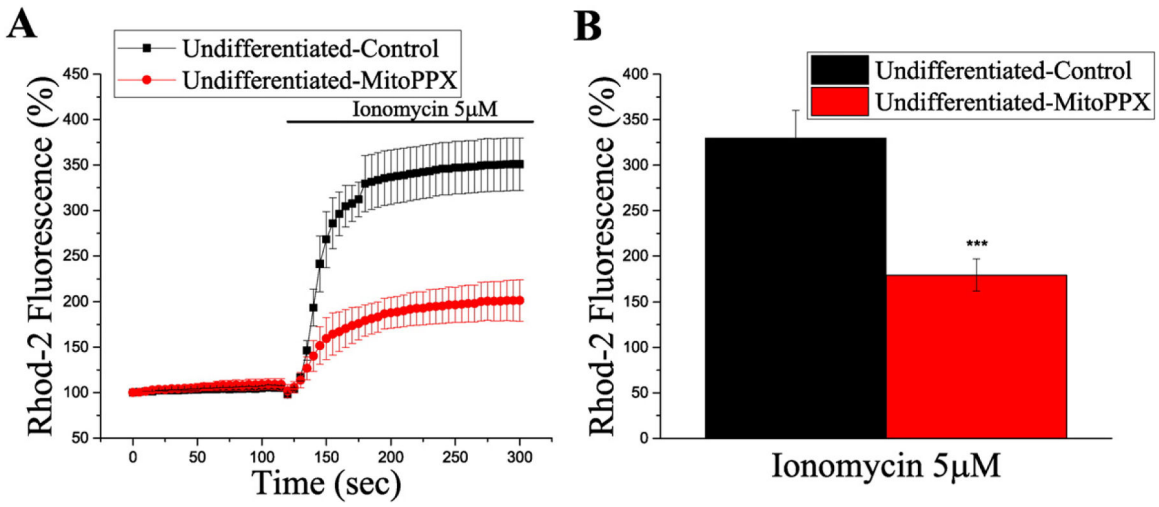

Fig. 4.

[Ca^{+2}]mito-free is reduced in HepG2 cells expressing mitochondrially-targeted PPX (mitoPPX). A. Graph showing real-time [Ca^{+2}]mito-free kinetics measured by Rhod-2 fluorescence, after the addition of ionomycin. Data collected from the same field for the two conditions. MitoPPX cells were identified by fluorescent GFP signal. Every point is the average signal from at least, ten individual cells from each group. Data is shown as mean ± SEM. B. Bar graph showing Rhod-2 fluorescence after 180 s of recording, (ionomycin was added at second 120), in transfected and control HepG2 undifferentiated cells. Data shows the average of at least ten cells per individual experiment from, at least, three independent experiments, mean ± SEM, Student's test: ***p ˂ 0.001.